Available online at www.sciencedirect.com
ScienceDirect
International Journal of Heat and Fluid Flow 28 (2007) 211–219
International Journal of HEAT AND FLUID FLOW
www.elsevier.com/locate/ijhff

Prediction of turbulent forced convection of a nanofluid in a tube with uniform heat flux using a two phase approach

A. Behzadmehr [a], M. Saffar-Avval [b,*], N. Galanis [c]

[a] Department of Mechanical Engineering, University of Sistan and Baluchestan, Zahedan, Iran
[b] Department of Mechanical Engineering, Amirkabir University of Technology, Hafez Avenue, P.O. Box 15875-4413, Tehran, Iran
[c] Département de génie mécanique, Université de Sherbrooke, Que., Canada

Received 21 May 2005; received in revised form 17 April 2006; accepted 21 April 2006
Available online 12 July 2006

Abstract

Turbulent forced convection heat transfer in a circular tube with a nanofluid consisting of water and 1 vol.% Cu is studied numerically. Two phase mixture model has been implemented for the first time to study such a flow field. A single phase model formulation, which has been used frequently in the past for heat transfer with nanofluids, is also used for comparison with the mixture model. The comparison of calculated results with experimental values shows that the mixture model is more precise than the single phase model. The axial evolution of the flow field and fully developed velocity profiles at different Reynolds numbers are also presented and discussed.

Keywords: Nanofluids; Mixture model; Two phase flow; Single phase model; Turbulent forced convection

1. Introduction

Low thermal conductivity of conventional heat transfer fluids such as water, oil, and ethylene glycol mixture is a serious limitation in improving the performance and compactness of many engineering equipments such as heat exchangers and electronic devices. To overcome this disadvantage, there is strong motivation to develop advanced heat transfer fluids with substantially higher conductivity.

An innovative way of improving the thermal conductivities of fluids is to suspend small solid particles in the fluid. Various types of powders such as metallic, non-metallic and polymeric particles can be added into fluids to form slurries. The thermal conductivities of fluids with suspended particles are expected to be higher than that of common fluids (Mansoori et al., 2002). An industrial application test was carried out by Liu et al. (1988) and the effects of flow rates on the slurry pressure drop and heat transfer behavior was investigated. In conventional cases the suspended particles are of μm or even mm dimensions. However, such large particles may cause severe problems such as abrasion and clogging. Therefore, fluids with suspended large particles have little practical application in heat transfer enhancement.

Nanofluids are a new kind of heat transfer fluid containing a small quantity of nanosized particles (usually less than 100 nm) that are uniformly and stably suspended in a liquid. The dispersion of a small amount of solid nanoparticles in conventional fluids changes their thermal conductivity remarkably. Compared to the existing techniques for enhancing heat transfer, the nanofluids show a superior potential for increasing heat transfer rates in a variety of cases. Choi (1995) quantitatively analyzed some potential benefits of nanofluids for augmenting heat transfer and reducing size, weight and cost of thermal apparatuses, while incurring little or no penalty in the pressure drop.

Researchers have demonstrated that oxide ceramic nanofluids consisting of CuO or Al_2O_3 nanoparticles in water or ethylene glycol exhibit enhanced thermal conductivity (Lee et al., 1999). A maximum increase in thermal

* Corresponding author. Tel.: +98 21 6405844; fax: +98 21 6419736.
E-mail address: mavval@aut.ac.ir (M. Saffar-Avval).

0142-727X/$ - see front matter © 2006 Elsevier Inc. All rights reserved.
doi:10.1016/j.ijheatfluidflow.2006.04.006

Nomenclature

a	acceleration
C_f	skin friction coefficient ($=\tau_w/0.5\rho V_0^2$)
C_p	fluid specific heat (J kg^{-1} K^{-1})
D	tube internal diameter (m)
g	acceleration of gravity (m s^{-2})
I	turbulent intensity
k	turbulent kinetic energy (m^2 s^{-2})
Pr	Prandtl number ($=\mu C_p/\lambda$)
q_w	uniform heat flux at the solid–fluid interface (W m^{-2})
r	radial coordinate (m)
Re	Reynolds number ($=V_0 D/v$)
T, t	time–mean and fluctuating temperature (K)
V, v	time–mean and fluctuating velocity (m s^{-1})
Z	axial coordinate (m)

Greek letters

ε	dissipation of turbulent kinetic energy (m^2 s^{-3})
Φ	volume fraction
λ	thermal conductivity (W m^{-1} K^{-1})
μ	dynamic viscosity (N s m^{-2})
v	kinematic viscosity (m^2 s^{-1})
ρ	density (kg m^{-3})

Subscripts

b	buoyancy
c	centerline
eff	effective
f	primary phase
k	the kth phase
m	mean
p	particle, secondary phase
s	solid
t	turbulent
w	wall
0	inlet condition
r	radial direction
z	axial direction
θ	tangential direction

Superscript

–	mean

conductivity of approximately 20% was observed in that study, having 4 vol.%. CuO nanoparticles with mean diameter 35 nm dispersed in ethylene glycol. A similar behavior has been observed in Al_2O_3/water nanofluid. For example, using Al_2O_3 particles having a mean diameter of 13 nm at 4.3% volume fraction increased the thermal conductivity of water under stationary conditions by 30% (Masuda et al., 1993). On the other hand, larger particles with an average diameter of 40 nm led to an increase of less than 10% (Lee et al., 1999). Furthermore, the effective thermal conductivity of metallic nanofluid increased by up to 40% for the nanofluid consisting of ethylene glycol containing approximately 0.3 vol.%. Cu nanoparticles of mean diameter less than 10 nm (Choi, 1995). Recently, a multi-wall nanotube in oil suspension (MWNT) yielded an extremely large increase in thermal conductivity (up to a 150% over the conductivity of oil) at approximately 1 vol.% nanotubes (Choi et al., 2001). This is the highest thermal conductivity enhancement ever achieved in a liquid.

Different concepts have been proposed to explain this enhancement in heat transfer. Xuan and Li (2000) and Xuan and Roetzel (2000) have identified two causes of improved heat transfer by nanofluids: the increased thermal dispersion due to the chaotic movement of nanoparticles that accelerates energy exchanges in the fluid and the enhanced thermal conductivity of nanofluids considered by Choi (1995). On the other hand Keblinski et al. (2002) have studied four possible mechanisms that contribute to the increase in nanofluid heat transfer: Brownian motion of the particles, molecular-level layering of the liquid/particle interface, heat transport in the nanoparticles and nanoparticles clustering. Similarly to Wang et al. (1999), they showed that the effects of the interface layering of liquid molecules and nanoparticles clustering could provide paths for rapid heat transfer.

Numerous theoretical and experimental studies have been conducted to determine the effective thermal conductivity of nanofluids. Most of these have been confined to liquids containing micro and milli-sized suspended solid particles. However, studies show that the measured thermal conductivity of nanofluids is much larger than the theoretical predictions (Choi et al., 2001). Many attempts have been made to formulate efficient theoretical models for the prediction of the effective thermal conductivity, but there is still a serious lack in this domain (Xue, 2003; Xuan et al., 2003).

As nanofluids are rather new, relatively few theoretical and experimental studies have been reported on convective heat transfer coefficients in confined flows. Pak and Cho (1998), Li and Xuan (2002) and Xuan and Li (2000, 2003) obtained experimental results on convective heat transfer for laminar and turbulent flow of a nanofluid inside a tube. They produced the first empirical correlations for the Nusselt number using nanofluids composed of water and Cu, TiO_2 and Al_2O_3 nanoparticles. The results indicate a remarkable increase in heat transfer performance over the base fluid for the same Reynolds number.

Convective heat transfer with nanofluids can be modeled using the two phase or single phase approach. The first provides the possibility of understanding the functions of both the fluid phase and the solid particles in the heat transfer process. The second assumes that the fluid phase

and particles are in thermal equilibrium and move with the same velocity. This approach is simpler and requires less computational time. Thus it has been used in several theoretical studies of convective heat transfer with nanofluids (Maige et al., 2004a,b; Roy et al., 2004; Khanfar et al., 2003). However, due to the fact that the effective properties of nanofluids are not known precisely, the numerical predictions of this approach are, in general, not in good agreement with experimental results. Therefore, the concerns in single phase modeling consist in selecting the proper effective properties for nanofluids and taking into account the chaotic movement of ultra fine particles. To partially overcome this difficulty, some researchers (for instance, Xuan and Li, 2000; Xuan and Roetzel, 2000) have used the dispersion model which takes into account the improvement of heat transfer due to the random movement of particles in the main flow.

Due to several factors such as gravity, friction between the fluid and solid particles and Brownian forces, the phenomena of Brownian diffusion, sedimentation, and dispersion may coexist in the main flow of a nanofluid. This means that the slip velocity between the fluid and particles may not be zero (Xuan and Li, 2000), therefore it seems that the two phase approach is better model to apply the nanofluid.

The two phase approach is based on an assumption of continuum phases. It provides a field description of the dynamics of each phase (Eulerian–Eulerian or two fluid model) or, alternatively, the Lagrangian trajectories of individual particles coupled with the Eulerian description of the fluid flow field (Fan and Zhu, 1998; Gidaspow, 1994). One of the foremost approaches in modeling two phase slurry flow is mixture theory, also called the theory of interacting continua (Ishii, 1975; Crowe et al., 1996; Manninen et al., 1996; Xu et al., 2004). The popularity of this latter approach in multiphase applications stems from the fact that it is simple in both theory and implementation. The required computations are relatively inexpensive. Furthermore, it is straight-forward to introduce a turbulence model into the mixture model, and most of all, it is reasonably accurate for a wide range of two phase flows.

In this paper, a two phase mixture model was applied to study the turbulent forced convection flow of a nanofluid in a uniformly heated tube. As far as we can ascertain, this is the first time that this approach has been used to study heat transfer involving nanofluids. The obtained results are compared with corresponding predictions from the single phase model.

2. Mathematical formulation and numerical procedure

2.1. Mixture model

The mixture model, based on a single fluid two phase approach, is employed in the simulation by assuming that the coupling between phases is strong, and particles closely follow the flow. The two phases are assumed to be interpenetrating, meaning that each phase has its own velocity vector field, and within any control volume there is a volume fraction of primary phase and also a volume fraction of the secondary phase. Instead of utilizing the governing equations of each separately, the continuity, momentum and energy equations for the mixture are employed. A nanofluid composed of water and Cu nanoparticles flowing in a long tube with uniform heating at the wall boundary is considered. Therefore, the dimensional equations for steady state mean conditions are

Continuity

$$\nabla \cdot (\rho_m V_m) = 0 \tag{1}$$

Momentum

$$\nabla \cdot (\rho_m V_m V_m) = -\nabla p_m + \nabla \cdot [\tau - \tau_t] + \rho_m g + \nabla \cdot \left(\sum_{k=1}^{n} \Phi_k \rho_k V_{dr,k} V_{dr,k} \right) \tag{2}$$

Energy

$$\nabla \cdot (\Phi_k V_k (\rho_k h_k + p)) = \nabla \cdot (\lambda_{eff} \nabla T - C_p \rho_m \overline{vt}) \tag{3}$$

Volume fraction

$$\nabla \cdot (\Phi_p \rho_p V_m) = -\nabla \cdot (\Phi_p \rho_p V_{dr,p}) \tag{4}$$

ρ_m is the mixture density

$$\rho_m = \sum_{k=1}^{n} \Phi_k \rho_k \tag{5}$$

where Φ is the volume fraction of phase k.

μ_m is the viscosity of the mixture that is obtained

$$\mu_m = \sum_{k=1}^{n} \Phi_k \mu_k \tag{6}$$

In Eq. (2), $V_{dr,k}$ is the drift velocity for the secondary phase k, i.e. the nanoparticles in the present study.

$$V_{dr,k} = V_k - V_m \tag{7}$$

$$\tau = \mu_m \nabla V_m \tag{8}$$

$$\tau_t = -\sum_{k=1}^{n} \Phi_k \rho_k \overline{v_k v_k} \tag{9}$$

The slip velocity (relative velocity) is defined as the velocity of a secondary phase (p) relative to the velocity of the primary phase (f)

$$V_{pf} = V_p - V_f \tag{10}$$

The drift velocity is related to the relative velocity

$$V_{dr,p} = V_{pf} - \sum_{k=1}^{n} \frac{\Phi_k \rho_k}{\rho_m} V_{fk} \tag{11}$$

The relative velocity is determined from Eq. (12) proposed by Manninen et al. (1996) while Eq. (13) by Schiller and

Naumann (1935) is used to calculate the drag function f_{drag}.

$$V_{pf} = \frac{\rho_p d_p^2}{18\mu_f f_{drag}} \frac{(\rho_p - \rho_m)}{\rho_p} a \tag{12}$$

$$f_{drag} = \begin{cases} 1 + 0.15 Re_p^{0.687} & Re_p \leqslant 1000 \\ 0.0183 Re_p & Re_p \succ 1000 \end{cases} \tag{13}$$

The acceleration (a) in Eq. (12) is

$$a = g - (V_m \cdot \nabla) V_m \tag{14}$$

An effective solid viscosity model in terms of solid volume fraction was obtained from the experimental work of Miller and Gidaspow (1992)

$$\mu_s = -0.188 + 537.42\Phi \tag{15}$$

Turbulence is modeled with the Launder and Spalding (1972) k–ε turbulence model for the mixture. It is expressed by Eqs. (16) and (17)

$$\nabla \cdot (\rho_m V_m k) = \nabla \cdot \left(\frac{\mu_{t,m}}{\sigma_k} \nabla k \right) + G_{k,m} - \rho_m \varepsilon \tag{16}$$

$$\nabla \cdot (\rho_m V_m \varepsilon) = \nabla \cdot \left(\frac{\mu_{t,m}}{\sigma_\varepsilon} \nabla \varepsilon \right) + \frac{\varepsilon}{k} (C_1 G_{k,m} - C_2 \rho_m \varepsilon) \tag{17}$$

where

$$\mu_{t,m} = \rho_m C_\mu \frac{k^2}{\varepsilon}, \quad G_{k,m} = \mu_{t,m} (\nabla V_m + (\nabla V_m)^T)$$
$$C_1 = 1.44, \quad C_2 = 1.92, \quad C_\mu = 0.09, \quad \sigma_k = 1, \quad \sigma_\varepsilon = 1.3 \tag{18}$$

The above governing equations are presented in cylindrical coordinates (R, θ, Z).

2.2. Single phase model

The single phase model, which has been used frequently for nanofluids, is also implemented to compare its predictions with the mixture model. The following equations represent the mathematical formulation of the single phase model for the governing equations and the turbulence modeling:

Continuity

$$\nabla \cdot (\rho_m V) = 0 \tag{19}$$

Momentum

$$\nabla \cdot (\rho_m V V) = -\nabla p + \nabla \cdot [\tau - \tau_t] + \rho_m g \tag{20}$$

Energy

$$\nabla \cdot (\rho_m V C_p T) = \nabla \cdot (\lambda_{eff} \nabla T - C_p \rho_m \overline{vt}) \tag{21}$$

where

$$C_{pm} = \sum_{k=1}^{n} \Phi_k C_{pk} \quad \text{and} \quad \lambda_{eff} = \sum_{k=1}^{n} \Phi_k \lambda_k \tag{22}$$

Launder and Spalding (1972) k–ε turbulence model is used for the turbulence modeling. It is expressed by the following two equations:

$$\nabla \cdot (\rho_m V k) = \nabla \cdot \left(\frac{\mu_{t,m}}{\sigma_k} \nabla k \right) + G_m - \rho_m \varepsilon \tag{23}$$

$$\nabla \cdot (\rho_m V \varepsilon) = \nabla \cdot \left(\frac{\mu_{t,m}}{\sigma_\varepsilon} \nabla \varepsilon \right) + \frac{\varepsilon}{k} (C_1 G_m - C_2 \rho_m \varepsilon) \tag{24}$$

The values of the constants are given in Eq. (18).

2.3. Boundary condition

The boundary conditions are expressed as follows:

- At the tube entrance ($Z = 0$):

$$V_z = V_0, \quad V_\theta = V_r = 0 \quad T = T_0 \quad I = I_0 \tag{25a}$$

Since the adopted model incorporates the assumption of turbulence isotropy, the corresponding turbulent kinetic energy is

$$k_0 = 1.5(I_0 V_0)^2 \tag{25b}$$

- At the tube outlet ($Z = L$):
  Zero diffusion flux in the axial direction with an overall mass balance correction
- At the fluid wall interface ($r = D/2$):

$$V_r = V_\theta = V_Z = 0, \quad k = \varepsilon = 0, \quad q_w = -\lambda_{eff} \frac{\partial T}{\partial r} \tag{26}$$

2.4. Numerical procedure

This set of coupled non-linear differential equations was discretized with the control volume technique. For the convective and diffusive terms the second order upwind method was used while the SIMPLE procedure was introduced for the velocity–pressure coupling. The discretization grid is uniform in the circumferential direction and non-uniform in the other two directions. It is finer near the tube entrance and near the wall where the velocity and temperature gradients are significant.

3. Validation and results

Several different grid distributions have been tested to ensure that the calculated results are grid independent. The selected grid consists of 160, 32 and 64 nodes in the axial, radial and circumferential directions, respectively. Fig. 1 shows the comparison of the velocity and temperature profiles for three different grid distributions. It is shown that the velocity and temperature profiles are independent of the number of grid points.

Two experimental results reported in the literature were used to validate the numerical procedure. In the first step, experimental measurements of gas–solid flow were considered to validate the numerical results obtained with the mixture model. Then experimental results for a nanofluid

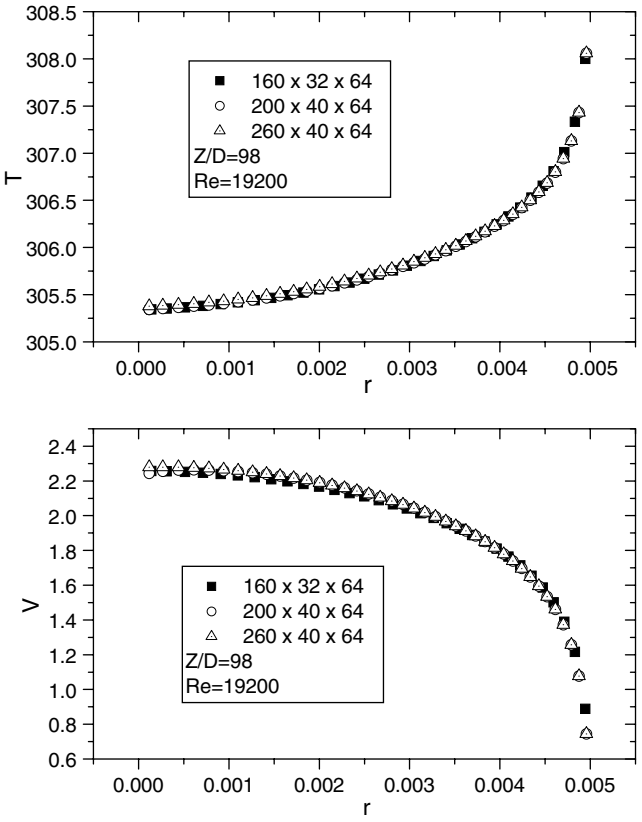

Fig. 1. Grid independence test.

were used to show the ability of the mixture model to predict the flow field of the nanofluids.

Fig. 2 shows the comparison of the experimental local heat transfer coefficient of a gas–solid flow (Depew and Farbar, 1963) with the numerical results for a particle diameter of 30 μm. The predicted axial evolution of the heat transfer coefficient using mixture model approach shows good agreement with the experimental results.

In order to show the validity of the mixture model and the numerical solution to predict heat transfer with a nanofluid the experimental works by Xuan and Li (2003) were chosen. The nanofluid consists of water and Cu with a volume fraction of 1.0%. Fig. 3 shows that the predicted Nusselt number is in good agreement with the experimental results for several different Reynolds number. This confirms the ability of the mixture model to predict nanofluid hydrodynamic and thermal fields. Furthermore, the calculated results for the same nanofluid based on the single phase and homogeneous flow are also illustrated in Fig. 3. The disagreement between the single phase predictions and the experimental results is considerably higher than the corresponding one for the mixture model. Therefore the mixture model predicts the experimental results more accurately than the single phase model (homogeneous model). Finally the experimental results of Fig. 3 clearly illustrate the heat transfer enhancement obtained by adding 1% nanoparticles (Cu) to water since the Nusselt number increases by more than 15%.

Results in the following paragraphs illustrate the effect of the Reynolds number on the turbulent forced convection flow characteristics of a nanofluid consisting of water and one percent volume fraction Cu with 42 nm mean diameter. The axial evolution of different hydrodynamics parameters as well as the fully developed velocity and particle concentration profiles are presented and discussed.

Fig. 4a shows the axial evolution of the non-dimensional turbulent kinetic energy at the tube centerline. These results clearly suggest the existence of a fully developed region for $Z/D > 50$. In the entrance region, the low inlet turbulent intensity remains constant for a short distance and then increases rapidly at $10 < Z/D < 20$. To understand this behavior we must note that turbulence is generated in the growing boundary layer and diffuses towards the center-

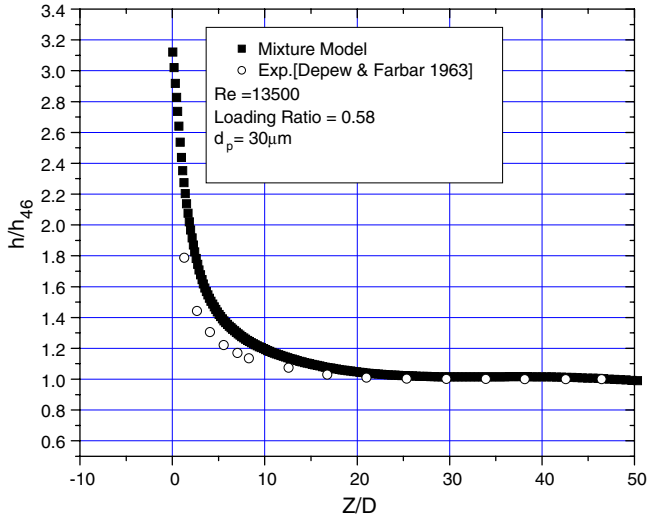

Fig. 2. Comparison of measured local heat transfer coefficients for a gas–solid two phase flow with calculated results using the two phase mixture model.

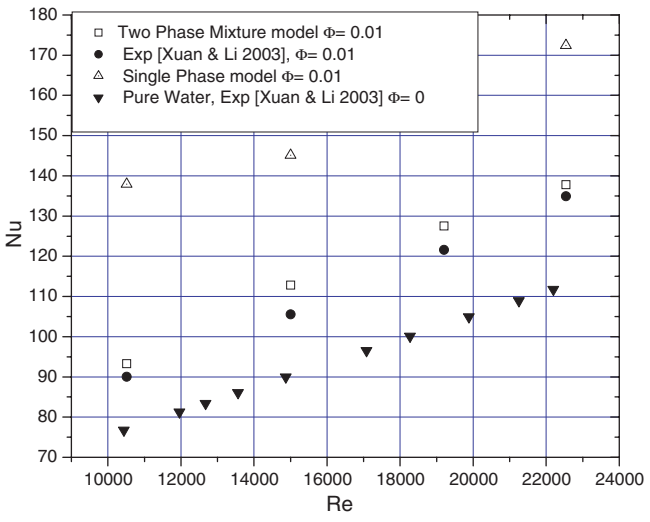

Fig. 3. Comparison of measured and calculated Nusselt numbers for a nanofluid flow.

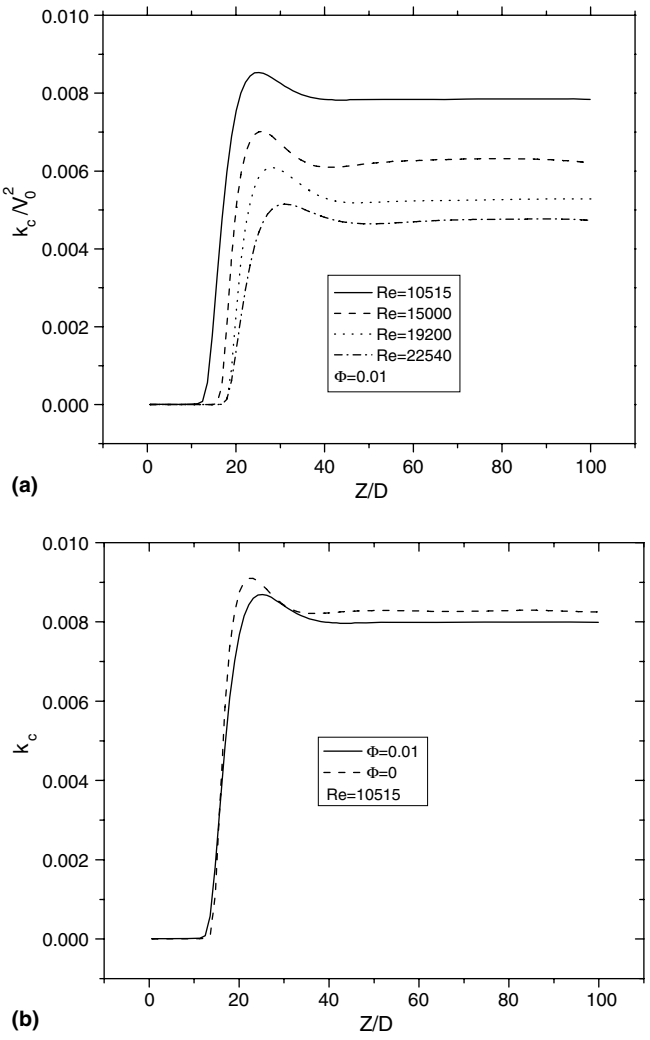

Fig. 4. Axial evolution of the centerline turbulent kinetic energy; (a) non-dimensional for different *Re*; (b) dimensional for pure water and nanofluid.

line. The position of the sudden turbulent kinetic energy increase in Fig. 4a corresponds to the position for which the diffusing turbulence reaches the tube centerline. As the Reynolds number increases, this position moves further downstream because the increasing axial momentum transports the generated turbulence in the flow direction. It is interesting to note that the maximum and fully developed values of the non-dimensional turbulent kinetic energy decrease as the Reynolds number increases. This is due to the fact that the corresponding velocity profiles become more uniform as *Re* increases (cf. discussion of Fig. 7a) and therefore turbulence generation near the tube axis decreases (cf. term *G*? in Eq. (16)). However, the detailed analysis of the results shows that the dimensional turbulent kinetic energy increases with increasing *Re* since V_0 increases.

Fig. 4b shows the axial evolution of k_c for the nanofluid flow as well as for pure water flow. Qualitatively the results are very similar. However, the nanofluid flow exhibits lower values of turbulent kinetic energy, which means that the solid particles absorbed some of the energy of the velocity fluctuations. Predictions with higher values of Φ confirmed this behavior. Thus higher values of the particle concentrations result in a lower value for k_c in the fully developed region (for example $k_c = 0.00767\ m^2/s^2$ for $\Phi = 2\%$ while it is $0.008\ m^2/s^2$ for $\Phi = 1\%$). In Fig. 4b since the concentration in the base fluid is low the amount of the absorbed energy is also low. Therefore, the difference between these two curves is small.

In order to be sure that this variation of k_c along the tube length is not due to the low value of the imposed turbulent intensity at the tube inlet ($I_0 = 0.1\%$), a high value of turbulent intensity at the tube inlet ($I_0 = 10\%$) was also considered. Fig. 5 shows the effect of the inlet turbulent intensity on the axial evolution of the centerline turbulent kinetic energy. The inlet condition has an effect which is limited to a few diameters downstream of the inlet. Downstream from $Z/D \approx 15$ the two curves show the same qualitative and quantitative behavior, particularly in the fully developed region.

The axial evolution of the velocity along the tube centerline is shown in Fig. 6a. Immediately after the tube inlet the boundary layer growth pushes the fluid towards the centerline region. This causes an increase of the centerline velocity up to approximately the position where k_c starts increasing (cf. Fig. 4a). Beyond this point, the higher turbulent kinetic energy results in a more uniform velocity profile and, therefore, the velocity at the centerline decreases in order to respect the continuity equation. These results confirm the existence of a fully developed region where the non-dimensional centerline velocity decreases as the Reynolds number increases (similarly to k_c, cf. Fig. 4a). The comparison with pure water flow is shown in Fig. 6b. It shows that the effect of the nanoparticles is not significant on the mean axial velocity and the general behavior is the same.

Fully developed velocity profiles are shown in Fig. 7. As expected, a higher Reynolds number results in a more uniform velocity profile.

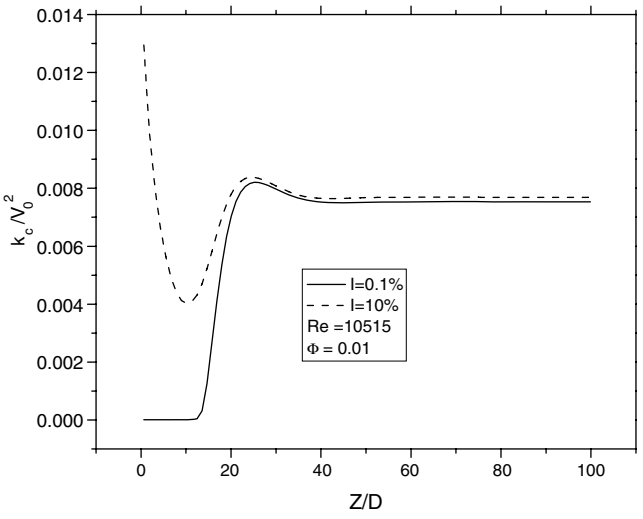

Fig. 5. Effect of the inlet turbulent intensity on the axial evolution of *k*.

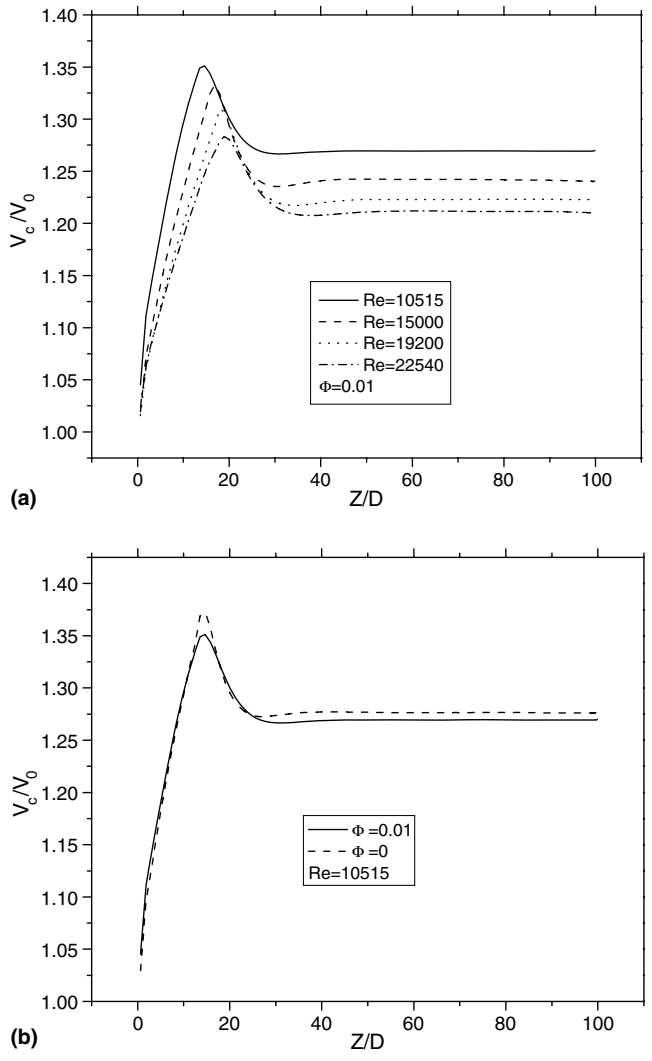

Fig. 6. Axial evolution of the centerline axial velocity; (a) effect of *Re*; (b) comparison for pure water and nanofluid.

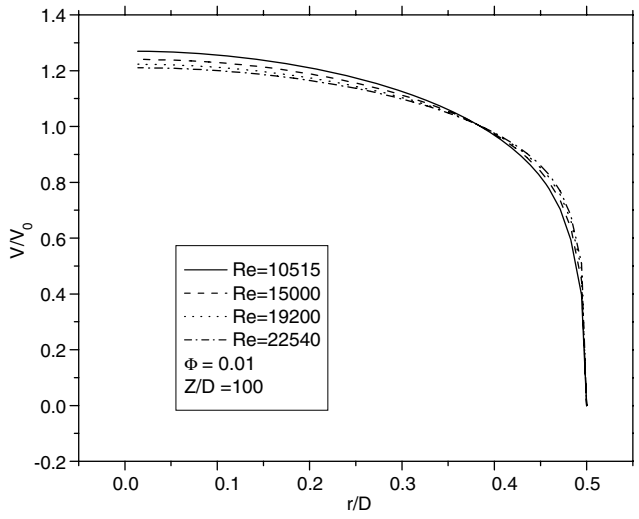

Fig. 7. Fully developed velocity profiles for different *Re*.

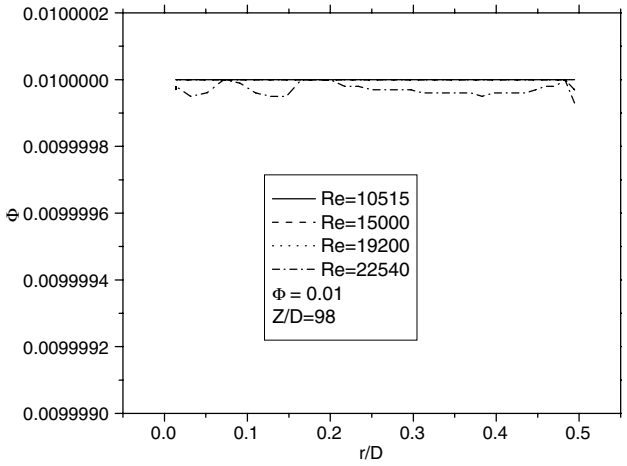

Fig. 8. Radial distribution of the fully developed particle volume fraction.

The radial variation of the particle concentration is shown in Fig. 8. It is uniform and constant for all Reynolds numbers except for the highest one. The constant value all along the tube diameter confirms that the distribution of the particles suspended in the fluid is completely uniform. Up to date all the numerical studies of nanofluid flow have been performed based on the assumption of uniform distribution of the nanoparticles in the base flow (see, for instance, Maige et al., 2004a,b). However, for the highest Reynolds number ($Re = 22{,}540$) this hypothesis is not completely valid according to the present results (qualitatively, since the equation for drift velocity was developed for μm and mm particles). Which means that for the high values of the $Re\,\Phi^{-1}$, the hypothesis of the uniform particles distribution which is implicitly included in single phase models may fail, and consequently the calculation results based on this hypothesis may not be correct.

The axial evolution of the local frictional coefficient is shown in Fig. 9a. Again the presence of the fully developed region is evident. As expected, the frictional coefficient decreases as the Reynolds number increases. Fig. 9b illustrates the axial evolution of this coefficient for a nanofluid and pure water flow ($\Phi = 0$). It shows that the nanoparticles do not have a significant effect on its value. This observation is also confirmed by the experimental results of Xuan and Li (2003).

Fig. 10 shows the evolution of the local Nusselt number along the tube length. It decreases, immediately after the tube inlet, and goes to a minimum value where the difference between the wall temperature and the bulk temperature are maximized. It goes to its asymptotic values at the fully developed region where the wall temperature and the bulk temperature are parallel. Increasing the particle concentration causes to increase the Nusselt number and thus the convection heat transfer coefficient.

4. Conclusion

Turbulent forced convection heat transfer in a circular tube with a nanofluid consisting of water and 1% Cu was

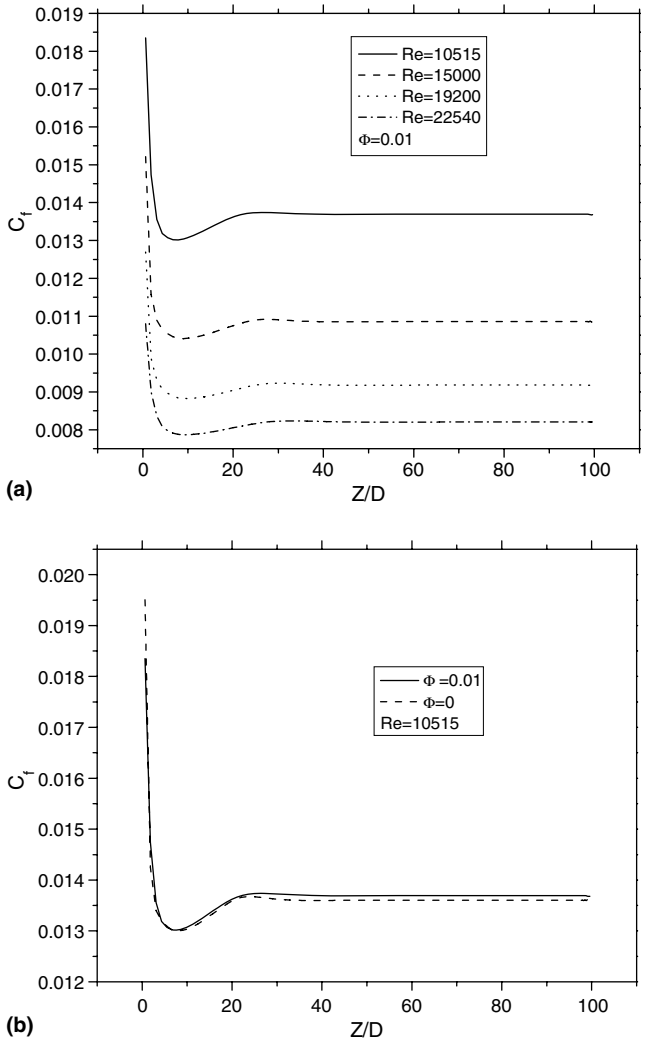

Fig. 9. Axial evolution of the local frictional coefficient; (a) effect of *Re*; (b) comparison for pure water and nanofluid.

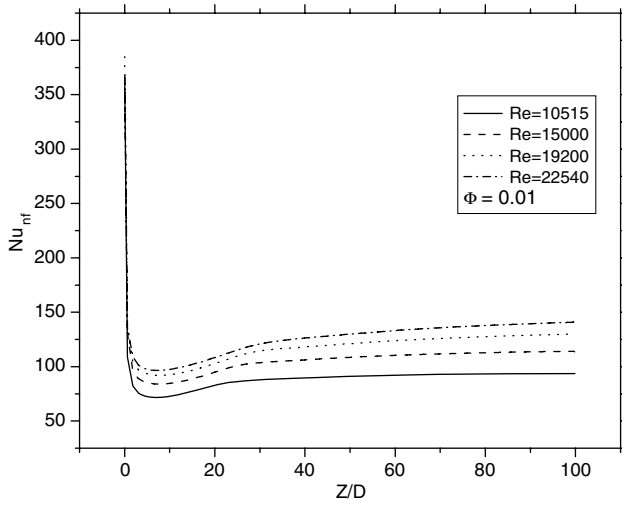

Fig. 10. Axial evolution of the Nusselt number.

studied numerically by using, for the first time, the two phase mixture model. The single phase model, which has been used frequently in previous studies of convection with nanofluids was also used for comparison with the mixture model. Comparisons of the Nusselt number predicted by these two models with corresponding experimental results show that the mixture model is more accurate than the single phase model. However, it seems that the accuracy of mixture model could improve by using suitable effective physical properties for nanofluid instead of volume weighted average of particle and fluid properties. Adding 1% nanoparticles (Cu), increases the Nusselt number more than 15% while it does not have any significant effect on the skin friction. It is shown that the particles concentration at high values of $Re\,\Phi^{-1}$ may not be uniform. Comparisons of heat transfer results for the nanofluid with those for the base fluid show that the particles can absorb the velocity fluctuation energy and reduce the turbulent kinetic energy.

Acknowledgments

The authors would like to acknowledge the Amirkabir University of Technology and Sistan and Baluchestan University for their financial support as well as the Natural Sciences and Engineering Research Council of Canada.

References

Choi, S.U.S., 1995. Enhancing thermal conductivity of fluid with nanoparticles, developments and applications of non-Newtonian flow. ASME, FED 231/MD 66, 99–105.

Choi, S.U.S., Zhang, Z.G., Yu, W., Lockwood, F.E., Grulke, E.A., 2001. Anomalous thermal conductivity enhancement in nanotube suspensions. Appl. Phys. Lett. 79 (14), 2252–2254.

Crowe, C.T., Troutt, T.R., Chung, J.N., 1996. Numerical models for two-phase turbulent flows. Ann. Rev. Fluid Mech. 28, 11–43.

Depew, C.A., Farbar, L., 1963. Heat transfer to pneumatically conveyed glass particles of fixed size. ASME Trans. (May), 164–172.

Fan, L.S., Zhu, C., 1998. Principle of Gas–Solid Flows. Cambridge University Press.

Gidaspow, D., 1994. Multiphase Flow and Fluidization. Academic Press.

Ishii, M., 1975. Thermo-Fluid Dynamic Theory of Two-Phase Flow. Eyrolles, Paris.

Keblinski, P., Phillpot, S.R., Choi, S.U.S., Eastman, J.A., 2002. Mechanisms of heat flow in suspensions of nano-sized particles (nanofluid). Int. J. Heat Mass Transfer 45, 855–863.

Khanfar, K., Vafai, K., Lightstone, M., 2003. Buoyancy driven heat transfer enhancement in a two dimensional enclosure utilizing nanofluids. Int. J. Heat Mass Transfer 46, 3639–3653.

Launder, B.E., Spalding, D.B., 1972. Lectures in Mathematical Models of Turbulence. Academic Press, London, England.

Lee, S., Choi, S.U.S., Li, S., Eastman, J.A., 1999. Measuring thermal conductivity of fluids containing oxide nanoparticles. J. Heat Transfer 121, 280–289.

Li, Q., Xuan, Y.M., 2002. Convective heat transfer performance of fluid with nanoparticles. In: Proc. 12th Int. Heat Transfer Conf., pp. 483–488.

Liu, K.V., Choi, S.U.S., Kasza, K.E., 1988. Measurement of pressure drop and heat transfer in turbulent pipe flows of particulate slurries. Argonne National Laboratory Report, ANL-88-15.

Maige, S.E. Nguyen, C.T., Galanis, N., Roy, G., 2004. Heat transfer enhancement in forced convection laminar tube flow by using nanofluids. ICHMT Int. Symp. Adv. Comput. Heat Transfer.

Maige, S.E., Nguyen, C.T., Galanis, N., Roy, G., 2004b. Heat transfer behaviors of nanofluids in a uniformly heated tube. Super Lattices Microstruct. 35 (3–6), 543–557.

Manninen, M., Taivassalo, V., Kallio, S., 1996. On the Mixture Model for Multiphase Flow, VTT Publications 288. Technical Research Center of Finland.

Mansoori, Z., Saffar-Avval, M., Basirat Tabrizi, H., Ahmadi, G., 2002. Modeling of heat transfer in turbulent gas–solid flow. Int. J. Heat Mass Transfer 45, 1173–1184.

Masuda, H., Ebata, A., Teramae, K., Hishinuma, N., 1993. Alteration of thermal conductivity and viscosity of liquid by dispersing ultra-fine particles (dispersions of γ-Al_2O_3, SiO_2, and TiO_2 ultra-fine particles). Netsu Bussei (Japan) 4, 227–233.

Miller, A., Gidaspow, D., 1992. Dense, vertical gas–solid flow in a pipe. AIChE J. 38 (11), 1801–1815.

Pak, B.C., Cho, Y.I., 1998. Hydrodynamic and heat transfer study of dispersed fluids with submicron metallic oxide particles. Exp. Heat Transfer 11 (2), 151–170.

Roy, G., Nguyen, C.T., Lajoie, P.R., 2004. Numerical investigation of laminar flow heat transfer in a radial flow cooling system with use of nanofluids. Supper Lattices Microstruct. 35, 497–511.

Schiller, L., Naumann, A., 1935. A drag coefficient correlation. Z. Ver. Deutsch. Ing. 77, 318–320.

Wang, X., Xu, X., Choi, S.U.S., 1999. Thermal conductivity of nanoparticle–fluid mixture. J. Thermophys. Heat Transfer 13, 474.

Xuan, Y.M., Li, Q., 2000. Heat transfer enhancement of nanofluids. Int. J. Heat Fluid Flow 21, 58–64.

Xuan, Y.M., Li, Q., 2003. Investigation on convective heat transfer and flow features of nanofluids. J. Heat Transfer 125, 151–155.

Xuan, Y.M., Roetzel, W., 2000. Conceptions for heat transfer correlation of nanofluids. Int. J. Heat Mass Transfer 43 (19), 3701–3707.

Xuan, Y.M., Li, Q., Hu, W., 2003. Aggregation structure and thermal conducting of nanofluids. AIChE J. 49 (4), 1038–1043.

Xue, Q.Z., 2003. Model for effective thermal conductivity of nanofluids. Phys. Lett. A 307 (5–6), 313–317.

Xu, J., Rouelle, A., Smith, K.M., Celik, D., Hussaini, M.Y., Van Sciver, S.W., 2004. Two-phase flow of solid hydrogen particles and liquid helium. Cryogenics 44, 459–466.